European Journal of Medicinal Chemistry 58 (2012) 12–21

Contents lists available at SciVerse ScienceDirect

European Journal of Medicinal Chemistry

journal homepage: http://www.elsevier.com/locate/ejmech

Original article

Synthesis of novel octa-cationic and non-ionic 1,2-ethanediamine substituted zinc (II) phthalocyanines and their *in vitro* anti-cancer activity comparison

Ao Wang [1], Li Zhou [1], Kelong Fang, Lin Zhou, Yun Lin, Jiahong Zhou, Shaohua Wei*

College of Chemistry and Materials Science, Jiangsu Key Laboratory of Biofunctional Materials, Nanjing Normal University, Wenyuan Road No.1, Nanjing 210046, PR China

ARTICLE INFO

Article history:
Received 9 May 2012
Received in revised form
12 September 2012
Accepted 13 September 2012
Available online 2 October 2012

Keywords:
Phthalocyanine
Photodynamic therapy
Photosensitizer
Singlet oxygen

ABSTRACT

Novel tetra-substituted zinc phthalocyanines (Pcs) bearing 1,2-ethanediamine group and the quaternized derivatives were synthesized and characterized. The photophysical and cellular properties of these Pcs were investigated. The results indicated that the quaternized ionic effect can greatly improve the water-solubility of Pcs and reduce their aggregation degree in aqueous solution. Comparative studies with quaternized phthalocyanine and its unquaternized counterpart have also demonstrated that the quaternary action on the molecules significantly enhances the fluorescence quantum yields, fluorescence lifetimes, efficiency of singlet oxygen production and, thereby, the *in vitro* photodynamic therapy efficacy.

1. Introduction

Photodynamic therapy (PDT) is a well-established modality for the treatment of a variety of localized tumors, including skin, mouth, esophageal, lung and bladder tumors [1,2]. Photodynamic therapy involves administration of a tumor localizing photosensitizing agent, followed by activation of the agent by light of a specific wavelength. This therapy results in a sequence of photochemical and photobiologic processes that cause irreversible photodamage to tumor tissues [3,4].

Pcs, which were first synthesized by chance in 1907, are remarkable macrocyclic compounds having magnificent physical and chemical properties [5,6]. Especially, owing to their high efficiency of singlet oxygen generation ability, extraordinary stability, and strong absorption in the phototherapeutic window (600–900 nm), Pc has been emerged as promising photosensitizers for PDT [7–9]. However, for most Pcs, low solubility and aggregation phenomena are observed in several organic media and in water, which have strong influence on their singlet oxygen ($^1O_2$) production efficiency, *in vivo* distribution and bioavailability. Above problems finally affect their application in PDT [10,11].

In order to decrease phthalocyanine aggregation and increase their water-solubility, several hydrophilic groups (e.g., polyethylene glycol, carbohydrates) and ionic substituent have been introduced at the macrocycle periphery [12–16]. Of particular interest are cationic Pcs, since such molecules have superior water-solubility, low aggregation degree and high cellular uptake efficiency [17–21]. Besides, According to the literature, the intracellular uptake efficacy and aggregation degree of Pcs are directly related to the number of positive ions in their structures [1,22,23].

Based on these conceptions, a new octa-cationic zinc phthalocyanine and other two unquaternized counterpart, as control, were synthesized. The properties of the three Pcs were discussed and compared. The results showed that octa-cationic zinc phthalocyanine not only have good solubility, low aggregation, high fluorescence quantum yields, high rate of singlet oxygen generation but also have high efficiency of intracellular uptake and *in vitro* anti-cancer activity. Above results indicated that the new octa-cationic zinc phthalocyanine offers potential as photosensitizer in PDT.

2. Experiments

2.1. Chemicals and reagents

4-nitrophthalonitrile was used after being recrystallized from methanol. All other necessary chemicals were of analytical grade obtained from commercial suppliers and were used without further purification unless otherwise stated. 1,8-diazabicyclo[5,4,0]-undec-

* Corresponding author. Tel./fax: +86 (0)25 85891761.
E-mail address: shwei@njnu.edu.cn (S. Wei).
[1] Both authors contributed equally to this work.

0223-5234/$ – see front matter © 2012 Elsevier Masson SAS. All rights reserved.
http://dx.doi.org/10.1016/j.ejmech.2012.09.038

7-ene (DBU), disodium salt of 9,10-anthracenedipropionic acid (ADPA) and CT-DNA were all purchased from established suppliers (Sigma–Aldrich, Acros) and used as received. All organic reagents were of analytical grade and were purified according to reported procedures [24] before use. TLC was performed on silica gel GF254 plates. Silica gel (300–400 mesh) was used for preparative column chromatography. Dulbecco's modified Eagle's medium (DMEM) was form Gibco.

2.2. Characteristics

The water-soluble Pcs were dissolved in water and in the case of Pcs insoluble in water, the stock solution was prepared in dimethyl sulfoxide (DMSO) and diluted with water to the final concentration for all experiments. Infrared spectra were measured in KBr pellets on IR-Spectrometer Nicolet Nexus 670. ^{1}H NMR and ^{13}C NMR spectra were recorded using a Bruker Advance 400 MHz NMR spectrometer. Elemental analyses were taken with Vario MICRO, Elementar. UV–vis spectra were recorded on spectrophotometer Cary 5000, Varian. Fluorescence spectra were carried out using Perkin Elmer LS 50B fluorescence spectrophotometer. Fluorescence quantum yields and lifetimes were recorded on FM-4P-TCSPC, Horiba Jobin Yvon. Cell morphology changes were observed under a Zeiss Observer fluorescence microscope. A 665 nm LED was used as light source.

2.3. Photostability assaying

The photostability of the three Pcs were investigated in water. And the decrease in the Q-band absorption of the phthalocyanine was monitored every 30 s using UV–vis spectrophotometer.

2.4. Singlet oxygen generation detection

The singlet oxygen ability of ZnPcs was carried out using disodium salt of 9,10-anthracenedipropionic acid (ADPA) as probe. Pcs (10×10^{-6} M) and ADPA (5.5×10^{-6} M) were mixed and irradiated. The reaction was monitored spectrophotometrically by measuring the decrease in optical density every 1 min at an absorbance maximum of 378 nm of ADPA.

2.5. Cell morphology

The cervical carcinoma cell line (HeLa) was maintained in Dulbecco's modified eagle's medium (DMEM) containing glucose supplemented with L-glutamine, pyridoxine hydrochloride, 110 mg L^{-1} sodium pyruvate, 0.1 mg mL^{-1} penicillin, 0.1 mg mL^{-1} streptomycin and 10% (v/v) fetal bovine serum (FBS), in a humidified atmosphere at 37 °C and 5.0% CO_2. After treatment with ZnPcs overnight and irradiating by light, cells were washed with phosphate buffered saline (PBS) three times and the cell morphology changes were observed under a fluorescence microscope.

2.6. Hoechst 33342 staining

Chromatin condensation was detected by nuclear staining with Hoechst 33342 [25]. After treatment with ZnPcs overnight and irradiating by light, cells were washed with phosphate buffered saline (PBS) three times and treated with 25 μg mL^{-1} Hoechst 33342 at 37 °C with 5% CO_2 in the dark for 30 min. Nuclear morphology change was observed under a fluorescence microscope.

2.7. Cellular uptake of ZnPcs *1*–*3* in HeLa cells

HeLa cells were incubated under the same experimental conditions with **ZnPc1** (5 μM), **ZnPc2** (5 μM) and **ZnPc3** (5 μM) for 24 h in the dark. After 24 h incubation, the drug concentration remaining in the medium was detected and calculated. All cellular uptake amounts were calculated according to the standard curves.

2.8. Intracellular ROSs detection by DCFH-DA

Intracellular generation of reactive oxygen species was measured by using an oxidation-sensitive fluorescent probe, 2′7′-dichlorofluorescin diacetate (DCFH-DA), whose oxidized form (2′7′-dichlofluorescein, DCF) is highly fluorescent [26,27]. HeLa cells were seeded in 6 well plates at 1×10^{5} mL^{-1} density. After incubation with ZnPcs (5 μM) for 24 h, cells were treated with 10 μM DCFH-DA. The control experiment used cells incubated in serum-free DMEM and DCFH-DA without ZnPcs. After 60 min incubation, cells were washed twice with PBS and then exposed to light for 5 min. After light exposure, cells were digested with pancreatic enzymes and dilute with 1 mL DMEM immediately, and the fluorescence of DCF was detected ($E_x = 488$ nm; $E_m = 530$ nm).

2.9. Dark cytotoxicity

For determination of dark cytotoxicity human embryonic kidney 293 cells (HEK 293) and HeLa cells were seeded into 96 well plates at a density of 5×10^{5} cells/cm^2 and incubated for 24 h in growth medium to allow for attachment. After 24 h, cellular survival was measured by using the classical [3-(4,5-dimethylthiazol-2-yl)-2,5-diphenyltetrazolium bromide] (MTT) colorimetric assay [28].

2.10. In vitro anti-cancer activity studies

For photo-induced anti-cancer experiments HeLa cells were incubated as described above, 24 h later, the old medium was replaced by fresh medium (without FBS) with **ZnPc1**, **ZnPc2** or **ZnPc3**, separately. Following 24 h incubation, the culture medium was replaced by FBS-free medium and rinsed for three times by PBS to remove adhered drugs. The cells were immediately exposed to light and after 24 h incubation, cells viability was measured as described above.

2.11. Statistical analysis

Student's *t*-test was used to analyze the differences in phototoxicity and mitochondrial membrane potential assay following treatment with free or HA-Tf. Experimental results are given as means ± SD of the indicated number of experiments. $P < 0.05$ was considered necessary for statistical significance.

3. Results and discussion

The synthetic procedure followed is outlined in Schemes 1 and 2.

3.1. Synthesis

3.1.1. N-tritylethane-1,2-diamine (*1*, Scheme 1)

A mixture of anhydrous ethylenediamine (1.5 g, 24.96 mmol) and finely ground anhydrous K_2CO_3 (3.45 g, 24.96 mmol) in CH_2Cl_2 (40 mL) was stirred under nitrogen at room temperature. Then, (chloromethanetriyl) tribenzene (3.48 g, 12.48 mmol) in CH_2Cl_2 (40 mL) was added dropwise to the solution over a period of 4 h, and stirring was continued overnight after the titration was completed. The formed solid material and K_2CO_3 were filtered off

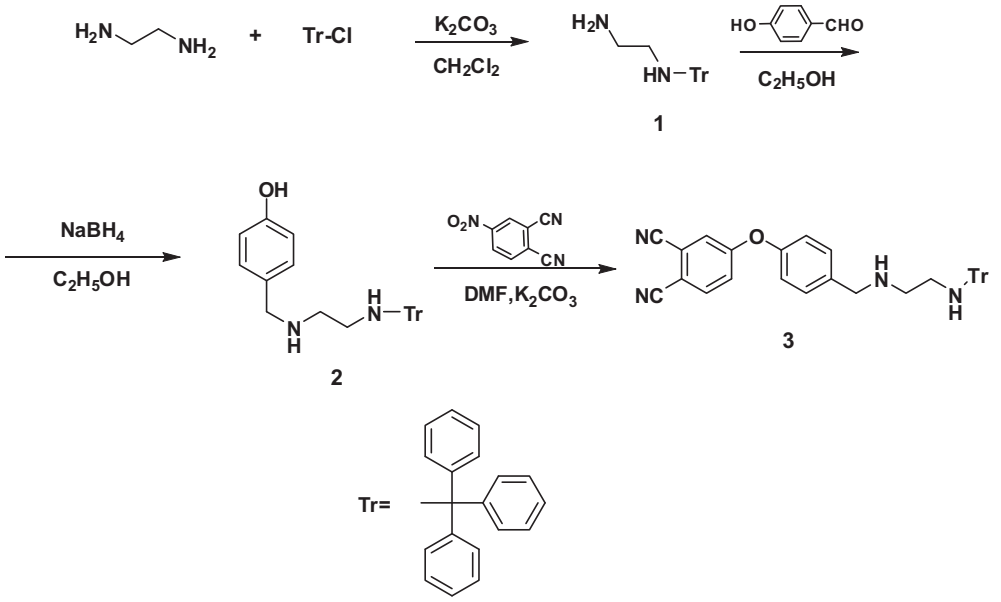

Scheme 1. Synthetic route to 4-(4-((2-(tritylamino)ethylamino)methyl)phenoxy)phthalonitrile.

and the filtrate was washed with water (3 × 100 mL). The solution was dried over anhydrous magnesium sulfate. After filtered, the solvent was evaporated in vacuum; the residue was purified by column chromatography with silica gel as column material and methanol/ethyl acetate (1:3) solvent system as elution. Yield: 3.39 g (90.0%). M.P. 83 °C. IR (KBr, cm^{-1}): 3420 (NH_2), 3370 (NH), 3290, 3090–3030 (Ph–H), 2930, 2850(CH_2), 1590, 1490, 1440, 756, 702. ^1H NMR (400 MHz, DMSO-d_6): δ (ppm) 7.41 (d, 6H, J = 7.66 Hz, Ar), 7.29 (t, 6H, J = 7.31 Hz, Ar), 7.16–7.2 (m, 3H, Ar), 2.63 (t, 2H, J = 6.04 Hz, CH_2), 2.45 (t, 2H, J = 5.64 Hz, CH_2). ^{13}C NMR (100 MHz, DMSO-d_6): δ (ppm) 146.7, 128.9, 128.1, 126.4, 70.6, 46.7, 42.3. Anal. Calcd. For $C_{21}H_{22}N_2$: C, 83.40; H, 7.33; N, 9.27. Found: C, 83.37; H, 7.37; N, 9.26.

3.1.2. 4-((2-(tritylamino)ethylamino)methyl)phenol (**2**, Scheme 1)

4-hydroxybenzaldehyde (1.87 g, 15.28 mmol) was slowly added to the solution of N-tritylethane-1,2-diamine (**1**) (4.20 g, 13.89 mmol) in dry C_2H_5OH (35 mL) at room temperature. About 10 min later, white precipitate appeared, and the reaction mixture was left stirred for another 3 h under ambient conditions. The reaction was monitored by TLC using methanol/ethyl acetate (1:3) solvent system for elution. The reaction mixture was poured into water (50 mL). The white solid material formed was filtered off and washed with absolute alcohol. Without further processing, the resulting precipitate was dissolved with dry C_2H_5OH (40 mL) and thereafter, $NaBH_4$ (0.58 g, 15.33 mmol) was added portion-wise over a period of 30 min. Then, the reaction mixture left to stir for a further 3 h at room temperature. At the end of this period, the resulting precipitate was filtered off and purified by column chromatographic separations with silica gel as column material and petroleum ether/ethyl acetate (1:3) solvent system as elution. Yield: 4.43 g (78.0%). M.P. 145 °C. IR (KBr, cm^{-1}): 3440 (OH), 3320 (NH), 3270, 3010–3070 (Ph–H), 2930, 2840 (CH_2), 1620, 1590, 1520, 1490, 1250, 750, 710. ^1H NMR (400 MHz, DMSO-d_6): δ (ppm) 9.18 (s, 1H, –OH), 7.40 (d, 6H, 7.92 Hz, Ar), 7.28 (t, 6H, 7.63 Hz, Ar), 7.17 (t, 3H, 7.24 Hz, Ar), 7.04 (d, 2H, 8.26 Hz, Ar), 6.67 (d, 2H, 8.31, Ar), 3.43 (s, 2H, $ArCH_2$), 2.59 (t, 2H, 5.85, CH_2), 2.09 (t, 2H, 9.33 Hz, CH_2). ^{13}C NMR (100 MHz, DMSO-d_6): δ (ppm) 156.4, 146.7, 131.4, 129.5, 128.8, 128.1, 126.5, 115.3, 70.7, 52.7, 49.0, 43.3. Anal. Calcd. For $C_{28}H_{28}N_2O$: C, 82.32; H, 6.91; N, 6.86. Found: C, 82.30; H, 6.92; N, 6.90.

3.1.3. 4-(4-((2-(tritylamino)ethylamino)methyl)phenoxy) phthalonitrile (**3**, Scheme 1)

Under nitrogen atmosphere, a mixture of 4-nitrophthalonitrile (0.94 g, 5.40 mmol) and finely ground anhydrous K_2CO_3 (1.24 g, 9.01 mmol) in dry DMF (10 mL) was stirred at room temperature. Then, 4-((2-(tritylamino)ethylamino)methyl)phenol (**2**) (1.84 g, 4.50 mmol) was added to the solution at once. The reaction mixture was heated to 40 °C, and left to stir for 5 h. During the whole process, the reaction was monitored by TLC using ethyl acetate/petroleum ether (1:2) solvent system for elution. After cooling to room temperature, the solution was filtered off. The filtrate was poured into CH_2Cl_2 (60 mL), then washed with distilled water (4 × 50 mL) and saturated brine (2 × 50 mL), and dried over anhydrous magnesium sulfate. The solvent was removed under vacuum and the crude product was purified by column chromatographic separations with ethyl acetate/petroleum ether (1:2) solvent system as elution. Yield: 2.20 g (91.3%). M.P. 52 °C. IR (KBr, cm^{-1}): 3425, 3320 (NH), 3050 (Ar–H), 2920, 2840 (CH_2), 2230 (CN), 1590, 1510, 1490, 1250, 708. ^1H NMR (400 MHz, DMSO-d_6): δ (ppm) 8.09 (d, 1H, 8.70, Ar), 7.75 (d, 1H, 2.18 Hz, Ar), 7.4 (t, 8H, 8.90 Hz, Ar), 7.35–7.27 (m, 7H, Ar), 7.20–7.12 (m, 5H, Ar), 3.6 (s, 2H, CH_2), 2.65 (t, 2H, 5.44 Hz, CH_2), 2.11 (s, 2H, CH_2). ^{13}C NMR (100 MHz, DMSO-d_6): δ (ppm) 161.8, 152.6, 146.7, 139.2, 136.7, 130.4, 128.9, 128.1, 126.5, 122.9, 122.1, 120.5, 117.1, 116.4, 115.8, 108.4, 70.7, 52.4, 49.3, 43.4. Anal. Calcd. For $C_{36}H_{30}N_4O$: C, 80.87; H, 5.66; N, 10.48. Found: C, 80.86; H, 5.67; N, 10.46.

3.1.4. 2(3), 9(10), 16(17), 23(24)-tetra-(((2-(tritylamino) ethylamino)methyl)phenoxy)phthalocyaninato-zinc (II) (***ZnPc1***, Scheme 2)

A mixture of anhydrous zinc acetate (0.09 g, 0.49 mmol), 4-(4-((2-(tritylamino)ethylamino)methyl)phenoxy)phthalonitrile (**3**) (0.42 g, 0.79 mmol) and DBU (0.4 g, 2.63 mmol) was stirred and heated at 140 °C in dry *n*-pentanol (10 mL) for 24 h under nitrogen atmosphere. After cooling to room temperature, the reaction solution was poured in to CH_3OH (60 mL). The deep blue solid product was precipitated and collected by filtration, then washed with H_2O and methanol till the filtrate was colorless. The green crude product was purified by passing through a silica gel column with firstly petroleum ether/ethyl acetate (1:3), then methanol/

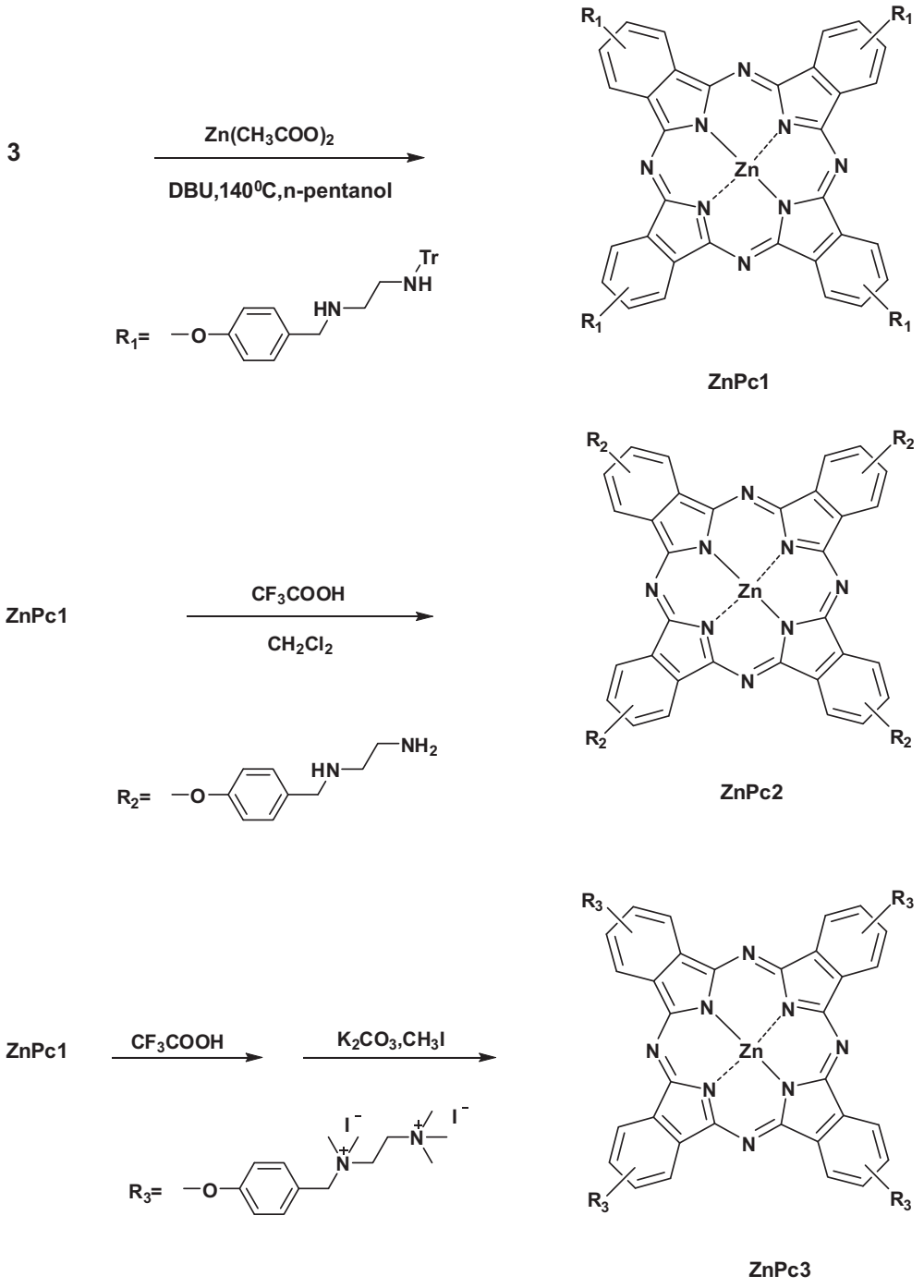

Scheme 2. Synthetic route to tetra-substituted zinc Pcs (**ZnPc1**, **ZnPc2** and **ZnPc3**).

CH_2Cl_2 (1:40) as elution. The blue fraction was collected, evaporated under vacuum, and vacuum-dried at 50 °C for 12 h to afford the product as a dark green solid. Yield: 0.27 g (62.36%). M.P. >200 °C. IR (KBr, cm^{-1}): 3450, 3060, 2930, 2840, 1710, 1600, 1480, 1230, 945, 708. ^{1}H NMR (400 MHz, DMSO-d_6) δ (ppm): 8.75–8.55 (br, 4H, Pc–H), 8.32 (s, 4H, Pc–H), 7.13–7.43 (br, 80H, Pc–H, Ar), 3.62 (m, 8H, CH_2), 2.71 (s, 8H, CH_2), 2.02 (s, 8H, CH_2). ^{13}C NMR (100 MHz, $CDCl_3$): δ (ppm) 146.2, 129.9, 129.8, 128.7, 128.1, 127.8, 127.6, 126.2, 120.3 (br), 70.8, 53.2, 52.9, 49.5, 46.2, 46.1, 43.1, 31.9, 29.7, 29.6, 29.4, 22.7, 14.1, 11.3. Anal. Calcd. For $C_{144}H_{120}N_{16}O_4Zn$: C, 78.47; H, 5.49; N, 10.17. Found: C, 77.67; H, 5.86; N, 9.80.

*3.1.5. 2(3), 9(10), 16(17), 23(24)-tetra-(((2-aminoethylamino) methyl)phenoxy)phthalocyaninato-zinc (II) (**ZnPc2**, Scheme 2)*

Under the condition of ice-water bath, **ZnPc1** (0.48 g, 0.22 mmol) and excess trifluoroacetic acid (TFA) (0.5 mL) were dissolved in CH_2Cl_2 (10 mL) and stirred for 1 h. Then, the reaction mixture was heated to room temperature and left to stir for another 2 h. The crude product was collected by filtration and washed successively with CH_2Cl_2. Thereafter, the green solid was dissolved in water and precipitated by adjusted pH to 9–10. The residue product collected by filtration was washed successively with water and methanol. The product was vacuum-dried at 50 °C for 12 h to afford the final

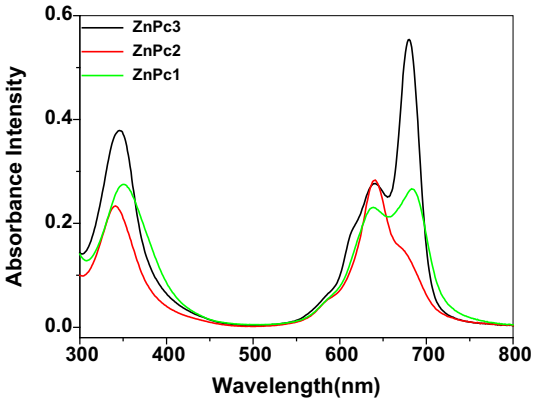

Fig. 1. Absorption spectra of the three Pcs (**ZnPc1**, **ZnPc2** and **ZnPc3**) in water. Concentration = 5×10^{-6} M.

compound as a dark green solid. Yield: 0.21 g (78.07%). M.P. >200 °C. IR (KBr, cm^{-1}): 3370, 2940, 2730, 1600, 1470, 1240, 1040, 945, 820. ^{1}H NMR (400 MHz, DMSO-d_6) δ (ppm): 9.25 (d, 4H, 17.4 Hz, Pc–H), 8.83 (s, 4H, Pc–H), 8.1 (s, 4H, Pc–H), 7.68–7.85 (m, 8H, Ar), 7.48 (d, 8H, 10.14 Hz, Ar) 4.33 (d, 8H, 10.52 Hz, CH_2), 3.31 (d, 8H, 5.2 Hz, CH_2), 3.23 (s, 8H, CH_2). ^{13}C NMR (100 MHz, D_2O): δ (ppm) 157.7 (br), 150.9 (br), 137.8 (br), 132.3, 131.3, 126.1, 124.3, 121.5, 120.0, 112.1 (br), 57.5, 51.2, 43.9, 35.7, 16.9, 16.8. Anal. Calcd. For $C_{68}H_{64}N_{16}O_4Zn$: C, 66.15; H, 5.22; N, 18.15. Found: C, 65.81; H, 5.56; N, 17.68.

3.1.6. *Quaternized 2(3), 9(10), 16(17), 23(24)-tetra-(((2-aminoethyl-amino)methyl)phenoxy)phthalocyaninato-zinc (II) (**ZnPc3**, Scheme 2) [29,30]*

A mixture of **ZnPc1** (0.43 g, 0.19 mmol) and excess trifluoroacetic acid (TFA) (0.5 mL) in CH_2Cl_2 was stirred at room temperature for 3 h. The solid was filtered and successively washed with CH_2Cl_2. The green solid product and K_2CO_3 (0.53 g, 3.80 mmol) were dissolved in CH_3OH (10 mL) and heated to boiling point of the solvent under nitrogen atmosphere. Then, excess CH_3I (1 mL, 16.00 mmol) were added, and the reaction mixture was left to stir for 24 h at refluxing. The crude solid green product was collected by filtration while hot, then washed by methanol (3 × 10 mL) and ethanol (5 × 10 mL) successively. The green product was dissolve in dry DMF (5 mL) and purified by filtering again to remove residual K_2CO_3. The solvent was removed under reduced pressure. The product was vacuum-dried at 50 °C for 24 h. The title product was obtained as a dark green solid. Yield: 0.40 g (80.8%). M.P. >200 °C. IR (KBr, cm^{-1}): 3427, 3011, 2586, 1601, 1475, 1234, 1069, 934, 751. ^{1}H NMR (400 MHz, DMSO-d_6) δ (ppm): 9.43 (t, 4H, 7.84 Hz, Pc–H), 9.07–9.01 (m, 4H, Pc–H), 7.93–8.00 (m, 4H, Pc–H), 7.82 (t, 8H, 9.87 Hz, Pc–H), 7.48–7.56 (m, 8H, Pc–H), 4.76 (d, 8H, 3.22 Hz, CH_2), 4.10 (s, 8H, CH_2), 4.01 (s, 8H, CH_2), 3.15–3.25 (br, 60H, CH_3). ^{13}C NMR (100 MHz, DMSO-d_6): δ (ppm) 159.9, 159.7, 157.6 (br), 152.9 (br), 140.4, 135.9, 135.8, 134.5, 124.8, 122.9, 122.7, 122.1, 119.4, 119.2, 119.1, 113.6, 113.1, 67.1, 57.5, 56.3, 53.7, 50.1, 19.0. Anal. Calcd. For $C_{88}H_{111}I_8N_{16}O_4Zn$: C, 41.65; H, 4.41; I, 40.01, N, 8.83. Found: C, 41.23; H, 4.76; N, 8.18.

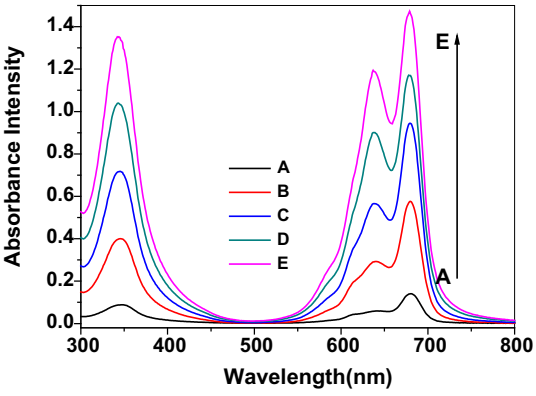

Fig. 2. Ground state electronic absorption spectra of **ZnPc3** at various concentrations: 1×10^{-6} (A), 5×10^{-6} (B), 9×10^{-6} (C), 13×10^{-6} (D), 17×10^{-6} (E) M in water.

Table 1
The monomer and aggregation electronic absorption data of **ZnPc3** in water.

Concentrations (M)	Absorbance (680 nm)	Absorbance (640 nm)	Proportion A_{680}/A_{640}
1×10^{-6}	0.1407	0.0591	2.38
5×10^{-6}	0.5757	0.2905	1.98
9×10^{-6}	0.9439	0.5651	1.67
13×10^{-6}	1.1695	0.9005	1.29
17×10^{-6}	1.4608	1.1939	1.22

3.2. *UV–vis spectral characterization*

The typical UV–vis spectra of the zinc Pcs usually exhibited characteristic monomer absorption band at ~680 nm while aggregate absorption band at 630–640 nm [31]. For PDT application, aggregation effect of Pcs always reduce their $^1O_2$ generation and, thereby, the *in vitro* anti-cancer activity. The UV–vis absorption spectra for **ZnPc1**, **ZnPc2** and **ZnPc3** are gathered in Fig. 1. Comparing studies indicated that only **ZnPc3** has strong monomer band at 680 nm in aqueous solution, which implies its strong photodynamic activity.

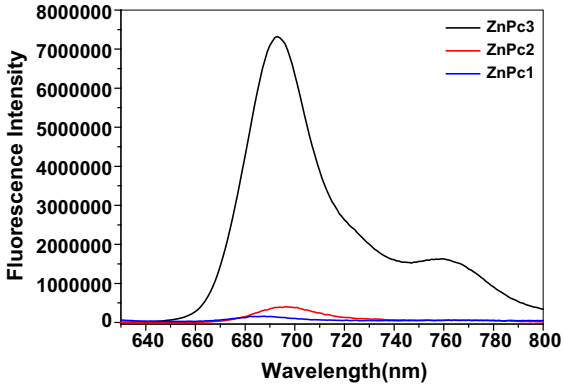

Fig. 3. Fluorescence spectra of the three Pcs (**ZnPc1**, **ZnPc2** and **ZnPc3**) in water. Concentration = 5×10^{-6} M; Excitation wavelengths: 600 nm.

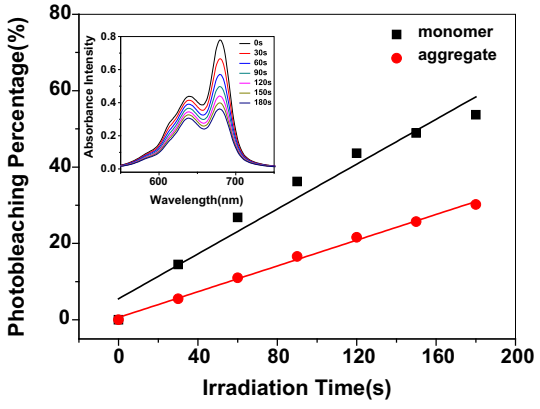

Fig. 4. Photo-bleaching of monomer (■) and aggregate (●) of **ZnPc3** measured by the decrease of the absorbance as the function of irradiation time (Inset: absorption spectra changes of **ZnPc3** irradiated by light in water; △ t = 30 s).

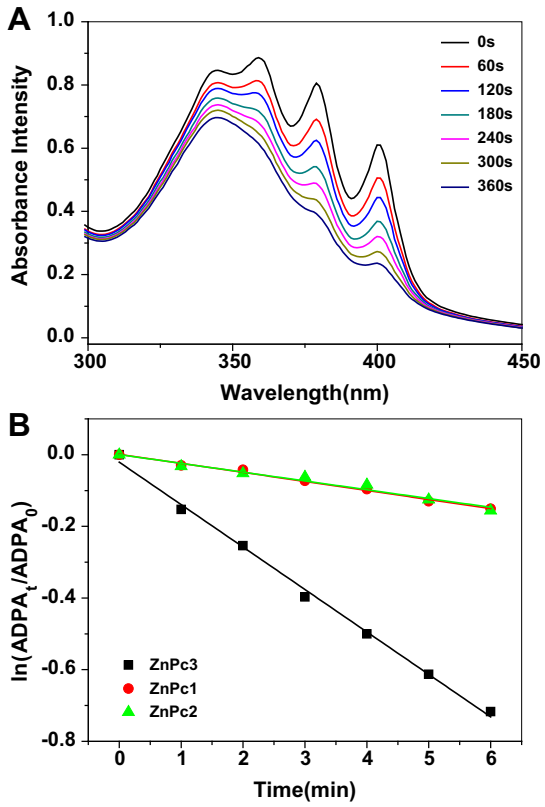

Fig. 5. (A) UV–vis spectrum for the determination of singlet oxygen quantum yields of **ZnPc3** in water use ADPA as quencher at the concentration of 10×10^{-6} M. (B) First order plots of ADPA absorbance *versus* time of the three Pcs.

Aggregation is usually depicted as a coplanar association of rings progressing from monomer to dimer and higher order complexes. It is dependent on the concentration, nature of the substituents, et al. [32]. In this study, the aggregation behavior of **ZnPc3** was investigated at different concentrations in water (Fig. 2). Due to the high value of the Q-band absorption, we were unable to obtain quantitative data for more concentrated solutions, however we found high monomer up to 1.7×10^{-5} M. Thus, it seems evident that the presence of eight positive charges efficiently prevents the aggregation of this phthalocyanine. Unlike to compound reported by Gabrio Roncucci et al. [33], as concentration was raised, the absorption at 680 nm and the band at 640 nm both became higher without new bands observed. The proportion of monomer/aggregation was shown in Table 1. The result indicated that although the eight positively charged quaternary ammonium groups give the dye a high solubility in water, increasing concentrations also enlarge the tendency of **ZnPc3** to form aggregates.

3.3. Fluorescence spectra and properties

In vivo and *in vitro* fluorescence detection, fluorescence usually employed to obtain information about photosensitizer localization and distribution as well as release from tissues [34].

Fluorescence emission spectra of the three zinc phthalocyanines were observed and collected in Fig. 3. In aqueous system, when excited at 600 nm, **ZnPc1** and **ZnPc2** showed very weak fluorescence while **ZnPc3** showed strong emission peak at 693 nm, same as other zinc Pcs [35]. This absence of fluorescence of the **ZnPc1** and **ZnPc2** dispersed in water can be due to either drug solvent interaction promoting nonradiative decay or quenching derived from self-aggregation of **ZnPc1** and **ZnPc2**. Aggregated metal Pcs are not known to fluorescence since aggregation lowers the fluorescence intensity of molecules through dissipation of energy [5]. But in the case of **ZnPc3**, the drug molecules can be existed as monomer, and therefore prevent a complete loss of fluorescence.

3.4. Photostability studies

Most photosensitizers will degrade during the process of PDT by photo-bleaching. In this process, the intensity of the absorption will decrease [36]. Thus, the stability of Pcs intended for use in PDT is especially important. In order to study the stability of the three ZnPcs, the photo-bleaching experiments were carried out and the Q-band absorption decreasing degrees were recorded. After irradiation, all the Pcs were bleached by light. Insert panel of Fig. 4 shows the photo-bleaching process of **ZnPc3** in water. Comparing results indicated that the aggregate is more stable than monomer under the irradiation (Fig. 4). Subsequent experiments prove that when the concentration increase, the photostability of **ZnPc3** also become better because many Pcs molecular were aggregate at high concentration condition. For **ZnPc1**, similar result that aggregate is more stable than monomer under the irradiation was got. The stability of monomer and aggregate of **ZnPc2** were not compared because there was

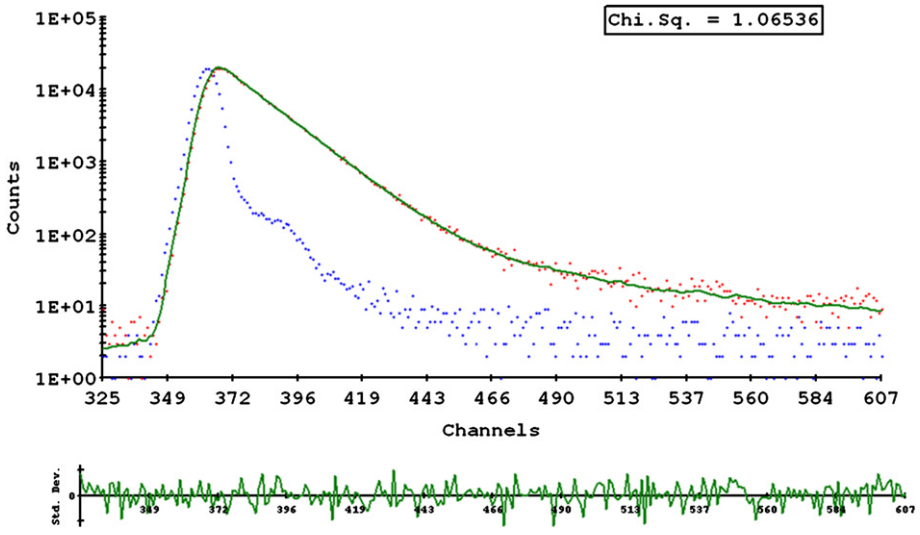

Fig. 6. The fluorescence lifetime of **ZnPc3** in H_2O at the concentration of 7×10^{-6} M (21.94787 ns = 1 channel).

Table 2
Cellular uptake percent of **ZnPc2** and **ZnPc3** with prolonged incubation time.

Compound	Cellular uptake percent (%)		
	2 h	4 h	24 h
ZnPc2	32.5	51.5	71.3
ZnPc3	52.9	61.2	86.5

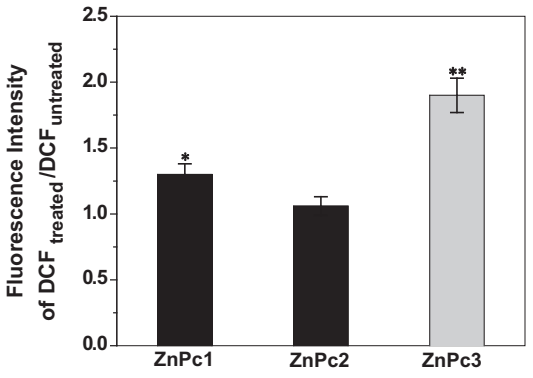

Fig. 7. Effect of Pcs **ZnPc1**, **ZnPc2** and **ZnPc3** on ROSs generation in HeLa cells ($^{*}P < 0.05$, $^{**}P < 0.01$ *vs*. Control; Control: cells were exposed to light without ZnPcs).

almost no monomer for **ZnPc2** in water. Besides, the stability of **ZnPc3** in comparison to **ZnPc1** and **ZnPc2** was also compared. The result showed that **ZnPc2** showed the best while **ZnPc3** the worse stability in water under irradiation (see Supporting information). The result can be attributed to the structure and exist states of Pcs (monomer or aggregate). It is also believed that photo-bleaching of Pcs is a singlet oxygen mediated process, since singlet oxygen is highly reactive and it can react with Pcs [31,32], which implies high singlet oxygen generation ability of **ZnPc3**.

3.5. Singlet oxygen generation ability

The singlet oxygen generation ability is an important indicator for the potential of photosensitizers in PDT [37]. Singlet oxygen can be detected using a chemical method by the photo-oxidation of ADPA to its endoperoxide derivative.

For all of the three ZnPcs, the absorption intensity of ADPA (λ = 378 nm) continuously decreased as the irradiation time increasing. The rate of singlet oxygen generation is calculated by the following equation described by Wei Tang et al. [38].

$$\ln\left([\mathrm{ADPA}]_t/[\mathrm{ADPA}]_0\right) = -kt$$

where $[\mathrm{ADPA}]_t$ and $[\mathrm{ADPA}]_0$ are the concentrations of ADPA after and prior irradiation, respectively. Values of k are the rate of singlet oxygen generation and t is the time of irradiation.

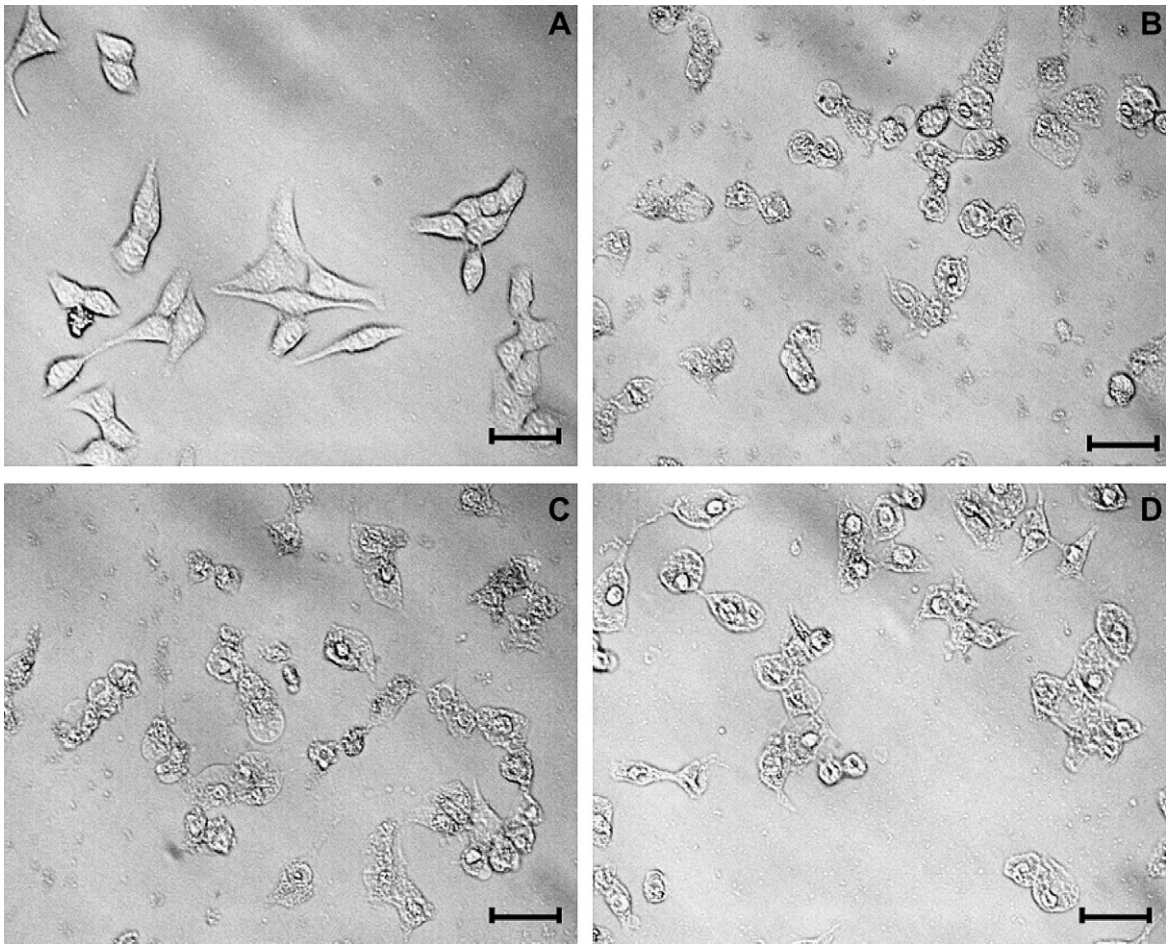

Fig. 8. Photograph showing morphology of normal HeLa cells (A) control untreated with photosensitizer and irradiated for 5 min; (B) treated with 5 μM **ZnPc1** irradiated for 5 min with LED light (λ_{ex} = 665 nm); (C) Treated with 5 μM **ZnPc2** irradiated for 5 min with LED light (λ_{ex} = 665 nm); (B) Treated with 5 μM **ZnPc3** irradiated for 5 min with LED light (λ_{ex} = 665 nm); 40 microscope objective. Bar = 100 μm.

In Fig. 5, higher singlet oxygen generation rate is observed for **ZnPc3** ($k_{ZnPc3} = 0.1185$) comparing with **ZnPc1** ($k_{ZnPc1} = 0.0253$) and **ZnPc2** ($k_{ZnPc2} = 0.0245$) indicated that the quaternarized ionic significantly increases the ability of ZnPcs to generate singlet oxygen. It is due to that quaternary increases the solubility of Pcs in the water and reduces their aggregation level at the same time. However, the rates of singlet oxygen generation of **ZnPc1** and **ZnPc2** are much lower than **ZnPc3**, which is in agreement with those previously reported for similar Pcs [23].

3.6. Fluorescence quantum yields (Φ_F) and lifetimes (τ_f)

The fluorescence quantum yield and lifetime are both important parameters for practical applications of fluorescence and reactive oxygen generation process. In our study, different from the common method [39], the fluorescence quantum yields of us obtained are absolute value rather than measured by comparison to a standard. **ZnPc1** has no fluorescence quantum yields, which can be attributed to fluorescence quenching of aggregation discussed above and the solvent effect. Higher fluorescence quantum yields were obtained for the quaternized **ZnPc3** (16.7%) in water compared to its unquaternized **ZnPc2** due to higher aggregation tendencies of **ZnPc2** in aqueous media.

The fluorescence lifetimes of the Pcs are obtained by the method of time-correlated single-photon counting (TCSPC). Fig. 6 shows the average fluorescence lifetime of **ZnPc3** in H_2O at the concentration of 7×10^{-6} M (**ZnPc3** as an example). The average fluorescence lifetimes of **ZnPc2** and **ZnPc1** were 2.87 ns and 2.40 ns, separately.

Besides, our results showed different from the literature which assert the fluorescence lifetime (τ_f) is directly related to that of fluorescence quantum yields (Φ_F); i.e. the longer the lifetime, the higher the quantum yield of fluorescence [37,6]. In our study, there are no positive correlation relationships between fluorescence lifetimes and fluorescence quantum yields. This may be attributed to the combined effects of structures, nature and environment of fluorescent groups, and so on, which are all of the crucial influencing factors of fluorescence lifetime and fluorescence quantum yield.

3.7. Cellular uptake of *ZnPc1*, *ZnPc2* and *ZnPc3* in HeLa cells

The relative uptake was quantified by comparison between the two water-soluble Pcs, **ZnPc2** and **ZnPc3**. Significant difference in cellular uptake efficiency was obtained from **ZnPc2** and **ZnPc3**. Taking into consideration that **ZnPc2** and **ZnPc3** both easily dissolved in water; these results possibly because of that the intracellular uptake efficiency of the cationic Pc (**ZnPc3**) was higher than non-ionic Pc (**ZnPc2**) due to the electronegative property of cancer cells (Table 2).

3.8. Intracellular production of reactive oxygen species (ROS)

It is well known that, upon illumination, photosensitizer is excited from the ground state to an excited state, generating free

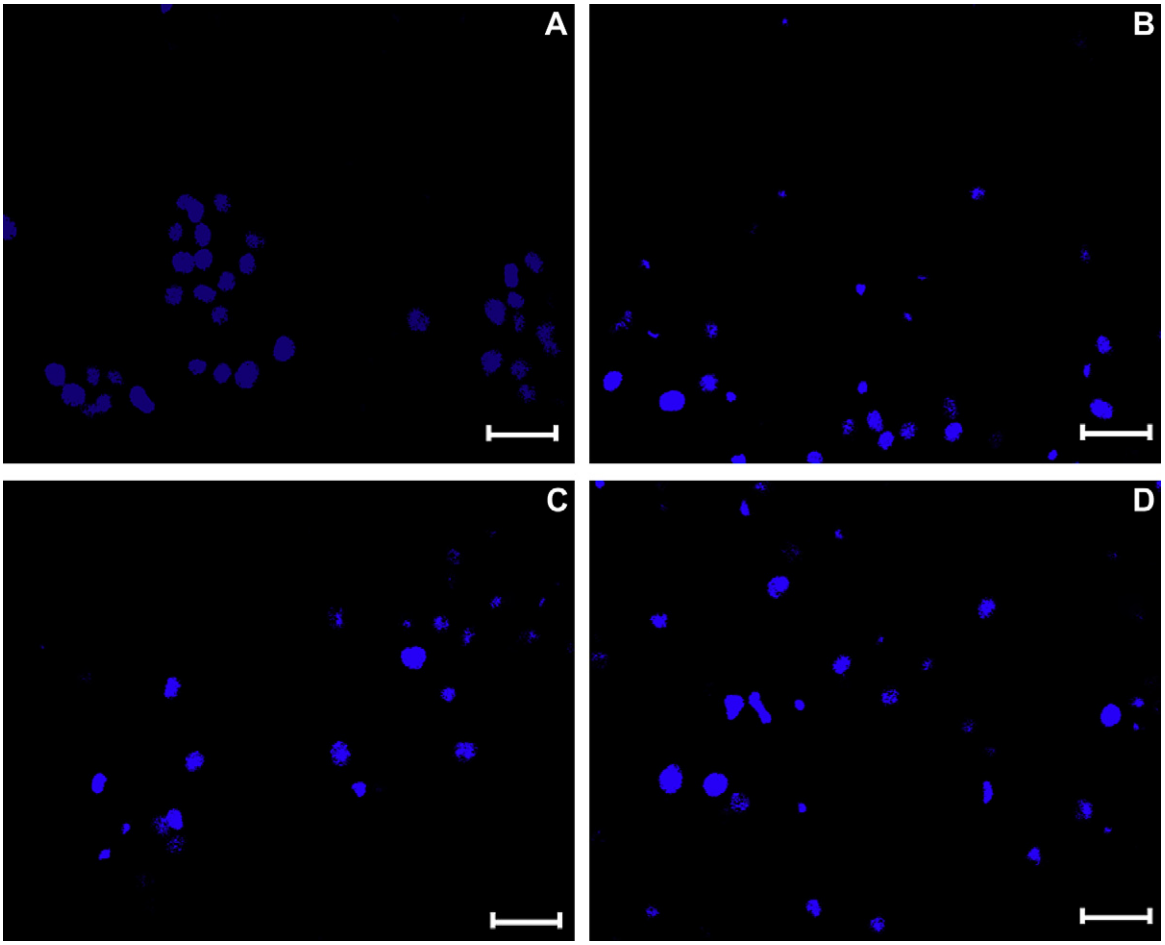

Fig. 9. Fluorescence micrographs of HeLa cells stained with Hoechst 33342. (A) Normal cells; (B) Cells treated with **ZnPc1** (5 μM) and 5 min of irradiation; (C) Cells treated with **ZnPc2** (5 μM) and 5 min of irradiation; (D) Cells treated with **ZnPc3** (5 μM) and 5 min of irradiation. Bar = 100 μm.

radicals and reactive oxygen species (ROSs), which are responsible for oxidative damage and cell death [40]. In order to evaluate the intracellular formation of ROSs after irradiation, HeLa cells pre-treated with **ZnPc1**, **ZnPc2** and **ZnPc3**, were loaded with the probe 2′7′-dichlorofluorescin-diacetate (DCFH-DA). After diffusing into cells, DCFH-DA is deacetylated by esterase and is then oxidized to the fluorescent 2′7′-dichlorfluorescein (DCF) in the presence of ROSs. As shown in Fig. 7, results are expressed as the ratio between DCF fluorescence, and represent the mean ± SD of three different experiments. The ROSs generation ability of **ZnPc3** was higher than **ZnPc2** and **ZnPc1**, which indicated that the *in vitro* photodynamic anti-cancer activity of **ZnPc3** should stronger than **ZnPc2** and **ZnPc1**.

3.9. Cell morphology

The morphology of HeLa cells was observed by microscopy after incubation with ZnPcs (5 μM) and irradiation for 5 min. Representative results are shown in Fig. 8. Microscopic observations showed that the HeLa cells changed their normal shape after photodynamic treatment. These results provided evidence about membrane deformation and an increase in the volume of cells indicating a higher fragility after the photodynamic action.

3.10. Hoechst 33342 staining

DNA damage is a very important index in PDT. The Hoechst 33342 is one part of a family of blue fluorescent dyes. Because the Hoechst can bind to DNA, so, it was used to assess changes in nuclear morphology. PDT process will damage tumor cells and induce DNA destruction in nuclear of cancer calls by activating photosensitizers by light. The results showed that there is no significant change in cell nuclear morphology, when the cells treated only with irradiation and the fluorescence of chromatin stained dimly and occupied the majority of the cell (Fig. 9A). In contrast, the cells treated with **ZnPc1** (Fig. 9B), **ZnPc2** (Fig. 9C) and **ZnPc3** (Fig. 9D) and irradiated by light showed obvious nuclear morphology changes, such as nuclear shrinkage, chromatin condensation, and fragmentation.

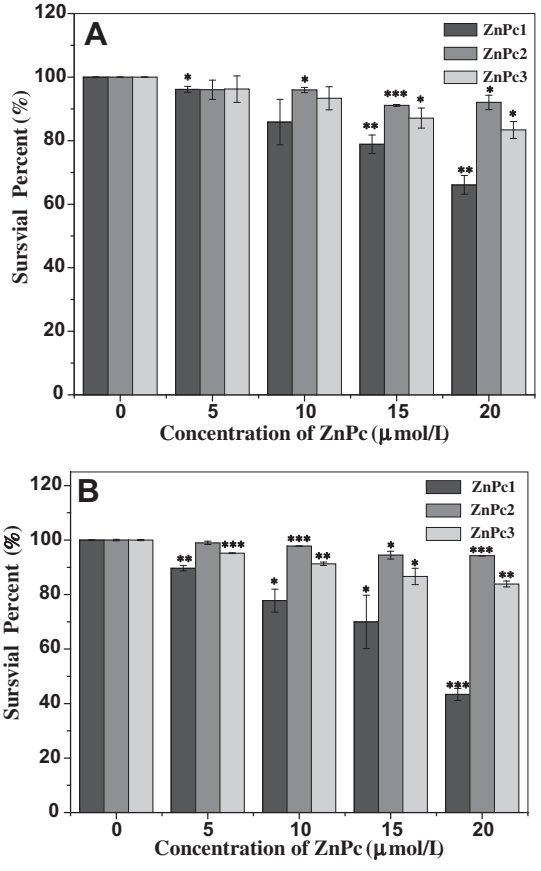

Fig. 10. Dark cell-viability assays with different drug doses of **ZnPc1**, **ZnPc2** and **ZnPc3** to HeLa (A) and HEK 293 (B) cells (*$P < 0.05$, **$P < 0.01$, ***$P < 0.001$ *vs.* Control; Control: cells were treated without ZnPcs).

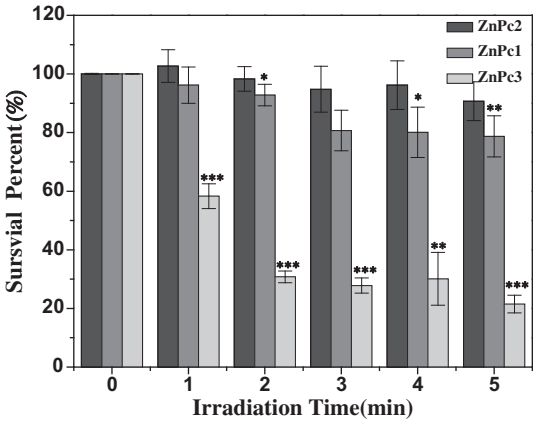

Fig. 11. Cell-viability assays with different light doses of **ZnPc1**, **ZnPc2** and **ZnPc3** (*$P < 0.05$, **$P < 0.01$ *vs.* Control; Control: cells were treated with ZnPcs but no irradiation).

3.11. Dark cytotoxicity

ZnPcs without illumination may have a cytotoxic effect, collectively referred to as dark cytotoxicity in the following. Fig. 10 shows the dark cytotoxic of **ZnPc1**, **ZnPc2** and **ZnPc3** in HeLa and HEK 293 cells. For **ZnPc2** and **ZnPc3** the cell-viability remains at about 95% of untreated controls up to a concentration of 5 μM while **ZnPc1** remains at about 89%. At concentrations higher than 20 μM the cell-viability decreases to lower than 65% (Fig. 10A) and 45% (Fig. 10B) for ZnPc1. The cell survival of **ZnPc2**- and **ZnPc3**-incubated cells remains higher than 80% up to a final concentration of 20 μM. Because of this, we settled on one concentration of 5 μM for the photodynamic reaction.

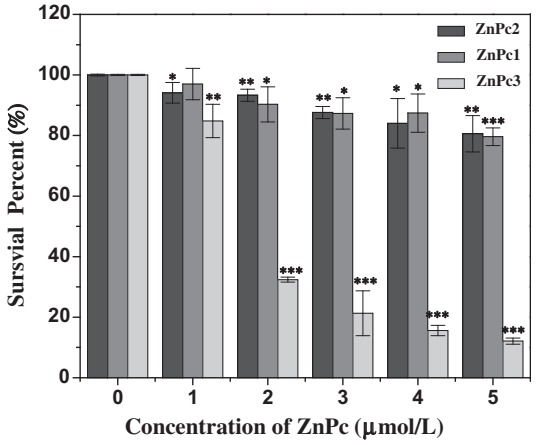

Fig. 12. Cell-viability assays with different drug doses of **ZnPc1**, **ZnPc2** and **ZnPc3** (*$P < 0.05$, **$P < 0.01$ *vs.* Control; Control: cells were exposed to light without ZnPcs).

3.12. Photo-induced anti-cancer activity

In order to determine the effect of light dose on **ZnPc1**-, **ZnPc2**- and **ZnPc3**-mediated PDT, HeLa cells were treated with 5 μM drugs, separately, and irradiation for 1–5 min. As showed in Fig. 11, after irradiation, **ZnPc1**, **ZnPc2** and **ZnPc3** all can induce tumor cell death but the anti-cancer activity of **ZnPc3** was much higher than **ZnPc1** and **ZnPc2**. After 5 min of irradiation, the survival percent of treated HeLa cells by **ZnPc1**, **ZnPc2** and **ZnPc3** were 90.7%, 78.7% and 21.5% respectively.

Furthermore, drug dose-dependent PDT efficacy was studied and Fig. 12 shows the cell survival percentage of treated HeLa cells with various drug dosages and subsequent irradiation with same light dose. As shown in Fig. 12, cell death can be observed for **ZnPc1**, **ZnPc2** and **ZnPc3**, as a function of the drug dose. However, the activity of **ZnPc3** was much higher than **ZnPc1** and **ZnPc2**.

4. Conclusion

We have prepared and characterized a series of novel zinc Pcs, including a quaternized and two unqutaternized Pcs. The pthotophysical property and *in vitro* anti-cancer activity were studied. Comparative studies with quaternized and unqutaternized Pcs have demonstrated that the quaternization effect on the Pcs molecules significantly enhances the water-solubility, the monomer percent, fluorescence intensity, efficiency of $^1O_2$ generation, intracellular uptake and, thereby, the *in vitro* PDT efficacy of the Pcs. Above results showed that the quaternized phthalocyanine has potential to be used as clinical photosensitizer for PDT.

Acknowledgements

This work was supported by the National Natural Science Foundation of China (20673058, 20973093), the Scientific Research Foundation of Nanjing Normal University (No. 2011103XG0249), and the Priority Academic Program Development of Jiangsu Higher Education Institutions (PAPD).

Appendix A. Supplementary data

Supplementary data related to this article can be found at http://dx.doi.org/10.1016/j.ejmech.2012.09.038.

References

[1] J. Marino, M.C. Garcia Vior, L.E. Dicelio, L. Roguin, J. Awruch, Eur. J. Med. Chem. 45 (2010) 4129–4139.
[2] H.R. Li, T.J. Jensen, F.R. Fronczek, M.G.H. Vicente, J. Med. Chem. 51 (2008) 502–511.
[3] T.J. Dougherty, C.J. Gomer, B.W. Henderson, G. Jori, D. Kessel, M. Korbelik, J. Moan, Q. Peng, J. Natl. Cancer Inst. 90 (1998) 889–905.
[4] G.A. Gauna, J. Marino, M.C.G. Vior, L.P. Roguin, J. Awruch, Eur. J. Med. Chem. 46 (2011) 5532–5539.
[5] M. Durmus, H. Yaman, C. Gol, V. Ahsen, T. Nyokong, Dyes Pigm. 91 (2011) 153–163.
[6] T. Nyokong, Coord. Chem. Rev. 251 (2007) 1707–1722.
[7] M. Camerin, M. Magaraggia, M. Soncin, G. Jori, M. Moreno, I. Chambrier, M.J. Cook, D.A. Russell, Eur. J. Cancer 46 (2010) 1910–1918.
[8] K.O. 'Riordan, O.E. Akilov, T. Hasan, Photodiagn. Photodyn. Ther. 2 (2005) 247–262.
[9] H.R. Li, N. Nguyen, F.R. Fronczek, M. Graca, H. Vicente, Tetrahedron 65 (2009) 3357–3363.
[10] K.T. de Oliveira, F.F. de Assis, A.O. Ribeiro, C.R. Neri, A.U. Fernandes, M.S. Baptista, N.P. Lopes, O.A. Serra, Y. Iamamoto, J. Org. Chem. 74 (2009) 7962–7965.
[11] B.D. Stasio, C. Frochot, D. Dumas, P. Even, J. Zwier, A. Muller, J. Didelon, F. Guillemin, M.L. Viriot, M.B. Heyob, Eur. J. Med. Chem. 40 (2005) 1111–1122.
[12] F. Dumoulin, M. Durmus, V. Ahsen, T. Nyokong, Coord. Chem. Rev. 254 (2010) 2792–2847.
[13] P.C. Lo, J.D. Huang, Y.Y.D. Cheng, E.Y.M. Chan, W.P. Fong, W.H. Ko, D.K.P. Ng, Chem. Eur. J. 10 (2004) 4831–4838.
[14] W. Liu, T.J. Jensen, F.R. Fronczek, R.P. Hammer, K.M. Smith, M.G.H. Vicente, J. Med. Chem. 48 (2005) 1033–1041.
[15] G.K. Karaoglan, G. Gumrukcu, A. Koca, A. Gul, Dyes Pigm. 88 (2011) 247–256.
[16] V. Mantareva, I. Angelov, V. Kussovski, R. Dimitrov, L. Lapok, D. Wohrle, Eur. J. Med. Chem. 46 (2011) 4430–4440.
[17] H. Cakc, A.A. Esenpnar, M. Bulut, Polyhedron 27 (2008) 3625–3630.
[18] B.S. Sesalan, A. Koca, A. Gul, Dyes Pigm. 79 (2008) 259–264.
[19] N. Kuznetsova, D. Makarov, O. Yuzhakova, A. Strizhakov, Y. Roumbal, L. Ulanova, A. Krasnovsky, O. Kaliya, Photochem. Photobiol. Sci. 8 (2009) 1724–1733.
[20] Z. Biyiklioglu, M. Durmus, H. Kantekin, J. Photochem. Photobiol. A: Chem. 211 (2010) 32–41.
[21] S.R. Wood, J.A. Holroyd, S.B. Brown, Photochem. Photobiol. 65 (1997) 397–402.
[22] M.R. Detty, S.L. Gibson, S.J. Wagner, J. Med. Chem. 47 (2004) 3897–3915.
[23] M. Kostka, P. Zimcik, M. Miletin, P. Klemera, K. Kopecky, Z. Musil, J. Photochem. Photobiol. A: Chem. 178 (2006) 16–25.
[24] D.D. Perrin, W.L.F. Armarego, Purification of Laboratory Chemicals, second ed., Pegamon Press, Oxford, 1989.
[25] Y.M. Zhao, L.N. Sun, H.Y. Zhou, X.L. Wang, Neurosci. Lett. 398 (2006) 22–27.
[26] Y.W. Yang, P.Y.J. Hsu, Biomaterials 29 (2008) 2516–2526.
[27] G. Spagnuolo, V. D'Anto, C. Cosentino, G. Schmalz, H. Schweikl, S. Rengo, Biomaterials 27 (2006) 1803–1809.
[28] A. Hussain, S. Gadadhar, T.K. Goswami, A.A. Karande, A.R. Chakravarty, Eur. J. Med. Chem. 50 (2012) 319–331.
[29] Y. Arslanoglu, T. Nyokong, Polyhedron 30 (2011) 2733–2739.
[30] P. Zimcik, V. Novakova, K. Kopecky, M. Miletin, R.Z.U. Kobak, E. Svandrlikova, L. Vachova, K. Lang, Inorg. Chem. 51 (2012) 4215–4223.
[31] M. Durmus, A. Erdogmus, A. Ogunsipe, T. Nyokong, Dyes Pigm. 82 (2009) 244–250.
[32] Z. Biyiklioglu, M. Durmus, H. Kantekin, J. Photochem. Photobiol. A: Chem. 222 (2011) 87–96.
[33] M.P.D. Filippis, D. Dei, L. Fantetti, G. Roncucci, Tetrahedron Lett. 41 (2000) 9143–9147.
[34] D.A. Fernfindez, J. Awruch, L.E. Dicelio, J. Photochem. Photobiol. B: Biol. 41 (1997) 227–232.
[35] E.N. Durantini, Bioorg. Med. Chem. 13 (2005) 3037–3045.
[36] J. Ferreira, P.F.C. Menezes, C. Kurachi, C. Sibata, R.R. Allison, V.S. Bagnato, Laser Phys. Lett. 5 (2008) 156–161.
[37] M. Durmus, V. Ahsen, J. Inorg. Biochem. 104 (2010) 297–309.
[38] W. Tang, H. Xu, R. Kopelman, M.A. Philbert, Photochem. Photobiol. 81 (2005) 242–249.
[39] M.C.G. Vior, L.E. Dicelio, J. Awruch, Dyes Pigm. 83 (2009) 375–380.
[40] W.M. Sharman, C.M. Allen, J.E. van Lier, Drug Discov. Today 4 (1999) 507–517.